Title

LEED INTENSITY ANALYSIS OF THE SURFACE STRUCTURES OF Pd(lll) AND OF CO ADSORBED ON Pd(lll) IN A (3 X 3)R300 ARRANGEMENT

Authors

Ohtani, H.
Hove, M.A. Van
Somorjai, G.A.

Publication Date

1987-04-01

LBL-23004
Preprint

Lawrence Berkeley Laboratory
UNIVERSITY OF CALIFORNIA

Materials & Chemical Sciences Division

Submitted to Surface Science

LEED INTENSITY ANALYSIS OF THE SURFACE STRUCTURES OF Pd(111) AND OF CO ADSORBED ON Pd(111) IN A ($\sqrt{3} \times \sqrt{3}$)R30° ARRANGEMENT

H. Ohtani, M.A. Van Hove, and G.A. Somorjai

April 1987

Prepared for the U.S. Department of Energy under Contract DE-AC03-76SF00098

DISCLAIMER

LEED Intensity Analysis of the Surface Structures of Pd(111) and of CO Adsorbed on Pd(111) in a $(\sqrt{3}x\sqrt{3})R30^\circ$ Arrangement

H. Ohtani, M. A. Van Hove, and G. A. Somorjai

Materials and Chemical Sciences Division, Lawrence Berkeley Laboratory
and Department of Chemistry, University of California, Berkeley, CA 94720

ABSTRACT

The surface structures of clean Pd(111) and of CO adsorbed on Pd(111) with a $(\sqrt{3}x\sqrt{3})R30^\circ$ periodicity at one-third monolayer coverage are investigated by dynamical LEED intensity analyses of measured I-V curves. The clean Pd(111) structure is confirmed to be close to the ideal bulk structure. Slight, possibly hydrogen-induced deviations are obtained for the interlayer spacings down to the fifth layer: $\Delta d_{12} = +0.03\pm0.03$Å, $\Delta d_{23} = -0.03\pm0.03$Å, and $\Delta d_{34} = \Delta d_{45} = +0.05\pm0.03$Å (positive values indicate expansion from the bulk spacing value). The CO molecules are favored to adsorb at fcc-type hollow sites with the C-O axis perpendicular to the surface. The optimal carbon-oxygen and metal-carbon bond lengths are 1.15 ± 0.05Å and 2.05 ± 0.04Å, respectively. This is the first LEED structure analysis of CO adsorbed at a hollow site on clean metal surfaces without coadsorbates.

1. Introduction

Recently surface crystallography by low energy electron diffraction (LEED) has been successful for determining the structures of molecular overlayers on single crystal surfaces. Adsorption structures have already been determined for CO molecularly adsorbed on Pt(111)[1], Rh(111)[2,3], Ru(0001)[4], Ni(100)[5–9], Cu(100)[5,6], and Pd(100)[10,11]. On these surfaces, the CO molecules have been confirmed to adsorb at 1-fold coordinated top sites or 2-fold coordinated bridge sites. Three-fold coordinated hollow sites occur less frequently: CO on Pd(111) is the only ordered case in which vibrational spectroscopy indicates[12,13] hollow sites (coadsorption also induces hollow sites for CO, as we have found with coadsorbed benzene[14,15,16]). For this reason and in preparation for other adsorbate studies on Pd(111), we have analyzed the structures of clean and CO-covered Pd(111).

The CO/Pd(111) system has been extensively studied in the past with a variety of techniques, including Thermal Desorption Spectroscopy (TDS)[17–22], work-function measurements[17,18], adsorption isotherms[17,18], LEED pattern analysis[12,13,17–19,23,24,28], molecular beam experiments[25], Ultraviolet Photoelectron Spectroscopy (UPS) [19,26], Angle-Resolved Photoelectron Emission Spectroscopy (ARPES)[27,28], Infrared Reflection Absorption Spectroscopy (IRAS)[12,13], Electron Energy Loss Spectroscopy (EELS)[23], Penning-Ionization Electron Spectroscopy (PIES)[26], and Secondary Ion Mass Spectroscopy (SIMS)[20].

These investigations have shown that CO is molecularly bonded to the Pd(111) surface through the carbon atom. The IRAS studies have shown the following dependence of the CO stretching frequency on the CO coverage(θ): At low

coverages a band appears at ~1820 cm^{-1}. This band gradually shifts up to ~1840 cm^{-1}, when a $(\sqrt{3}x\sqrt{3})R30°$ LEED pattern is observed at θ=1/3. Then this band moves quickly to ~1920 cm^{-1} by θ=0.4. For θ=0.5, the frequency is ~1940cm^{-1}. At higher coverages, a second band appears above 2000 cm^{-1}. According to the site assignments used in metal-carbonyl clusters, these results suggest that CO molecules are adsorbed on hollow sites up to θ=1/3, on bridge sites at θ=1/2, and on both bridge and top sites at higher coverages.

However, since the CO stretching frequency is affected by intermolecular interactions and the interaction between CO and metal, one cannot infer definitively from the C-O stretching frequency (1840cm^{-1}) whether CO molecules are adsorbed at hollow sites or at bridge sites. LEED can independently verify the site assignment. Furthermore, two inequivalent hollow sites are available on the Pd(111) surface, namely the fcc hollow site and the hcp hollow site (a hcp hollow site has a 2nd layer atom at the bottom of the hollow, while a fcc hollow site does not have one). Vibrational spectroscopy can not distinguish CO molecules adsorbed at these two different hollow sites, whereas LEED can. In addition, LEED can yield bond lengths and bond angles.

We report here the first study of the structure of Pd(111)-$(\sqrt{3}x\sqrt{3})R30°$-CO by dynamical LEED analysis. We not only verify the CO adsorption site, but also analyze the detailed bond lengths. These results can be useful for interpreting various kinds of spectroscopic data, such as IRAS, UPS, ARPES, EELS, and for better understanding of CO chemisorption on transition metals in general.

We also report here a detailed dynamical LEED analysis of the clean Pd(111) surface. This will be of value in various planned structural determinations involving a series of molecules adsorbed on this substrate, starting with the CO structure examined here. The structure of clean Pd(111) has already been studied by LEED intensity analysis[29,30] and High-Energy Ion Scattering (HEIS)[31,32]. All these studies have yielded the ideal structure of the truncated bulk. To our knowledge, however, no detailed structure determination to explore the surface relaxation has been performed on this surface.

2. Experiment

Experiments were performed in an ion-pumped, stainless steel UHV system, equipped with a quadrupole mass spectrometer, an ion bombardment gun, and a four-grid LEED optics. An off-axis electron gun, and the LEED optics were used for Auger electron spectroscopy. We used a palladium crystal of dimension, 6mm x 8 mm x 0.45 mm, spot-welded to tantalum support wires. The crystal could be cooled to $\sim$ 140 K by conduction from a pair of liquid nitrogen cold fingers or heated resistively to $\sim$ 1500 K. Temperatures were measured by a 0.005" chromel-alumel thermocouple spot-welded to one edge of the palladium crystal. The system base pressure was in the 10^{-10} torr range. H_2 and CO were the main components of the residual gas.

The LEED optics and vacuum chamber were enclosed by two sets of Helmholtz coils to minimize the magnetic field near the crystal. These coils were adjusted until there was no significant deflection of the specularly-reflected beam

over the 20 to 300 eV energy range used for LEED intensity vs. energy (I-V) measurements. There were no exposed insulators or ungrounded conductors in the vicinity of the crystal in order to minimize electrostatic fields. The LEED electron gun was operated in the space-charge limited mode, so that the beam current increased monotonically and approximately linearly over the voltage range used. At 200 eV the beam current was $\sim 4.0\mu$-amps. The intensity-energy curves were normalized with respect to incident beam current. The crystal was mounted on a manipulator capable of independent azimuthal and co-latitude rotations. The crystal surface was oriented with the (111) face perpendicular to the azimuthal rotation axis as determined by visual comparison of the intensities of symmetry related substrate beams. It is possible to see deviations from normal incidence of less than 0.2° with this method. The accuracy of the orientation was confirmed by the close agreement of I-V curves for symmetry-related beams. The off-normal incidence angles were set by rotating the crystal away from the experimentally determined normal-incidence position using a scale inscribed on the manipulator.

LEED data were collected using a high-sensitivity vidicon TV camera with a f/.85 lens. The data were recorded on video tapes, and the diffraction patterns were analyzed using a real-time video digitizer interfaced to an LSI-11 microcomputer[33]. Sixteen consecutive video frames at constant energy were summed to improve the signal/noise ratio, and an image recorded at zero beam voltage was subtracted to correct for the camera dark current and stray light from the LEED screen or filament. After such analysis at each energy, I-V curves were generated

by a data reduction program that locates diffraction spots in the digitized image, integrates the spot intensity, and makes local background corrections[34].

Sample Preparation

The major impurities in the Pd(111) crystals were sulfur and carbon. These were removed by several cycles of oxidation ($P_{O2} = 5x10^{-7}$torr, 400C) and 500 eV argon ion bombardment ($P_{Ar} = 5x10^{-5}$torr, both at room temperature and at 600C) followed by annealing at 500C. Right before the experiment, the crystal was flashed to 600C to desorb adsorbed CO and H originating from the background gas in the UHV chamber and to remove any residual carbon by diffusion into the bulk[35]. The surface cleanliness was checked by AES. The clean Pd(111) surface showed a sharp (1x1) LEED pattern with very low background intensity [Fig1.a]. Once the cleaning procedure was established, we no longer took Auger spectra before the LEED experiments so as to avoid possible contamination due to the electron-beam decomposition of residual gas on the surface.

The $(\sqrt{3}x\sqrt{3})R30°$-CO pattern was produced by exposing the clean Pd(111) to a nominal $8x10^{-9}$ torr of CO for 100 sec at room temperature. The crystal was located 10 cm away from a stainless steel doser tube 0.15 cm in diameter. A bright $(\sqrt{3}x\sqrt{3})R30°$ pattern was obtained reproducibly [Fig1.b]. The TDS (at mass 28) showed a single peak at 480K with heating rate ~15K/s. This implies that most of the CO molecules adsorb at one kind of site at this coverage. At higher coverages, a second peak appears at lower temperature, as reported before[19–22].

I-V Curve Measurement

The I-V data for the clean Pd(111) structure were collected at normal incidence and with the incident electron beam rotated 5 ° from normal incidence toward both the [1, 1, $\bar{2}$] and [$\bar{1}$, $\bar{1}$, 2] directions, which can be labeled (θ, ϕ) = (5 °, 0 °) and (5 °, 180 °), respectively; these directions of tilt maintain one mirror plane of symmetry. The energy range used was 20-300eV. The normal-incidence data set has 5 independent beams over a cumulative energy range of 700eV. The (5 °, 0 °) and (5 °, 180 °) data sets have 11 and 10 independent beams respectively, and each has a cumulative energy range of 1300eV.

The I-V data for the Pd(111)-($\sqrt{3}$x$\sqrt{3}$)R30 °-CO structure were collected with the same incident electron angles as used for clean Pd(111). The energy range used was 20-200eV. The normal-incidence data set has I-V curves for 8 independent beams over a cumulative energy range of 700 eV. The (5 °, 0 °) and the (5 °, 180 °) data sets have 17 and 12 independent beams and cumulative energy ranges of 1350 and 1200 eV, respectively. Both the normal-incidence data and the (5 °, 0 °) data are averages of two independent experiments.

The final I-V curves were obtained by averaging symmetrically equivalent beams. Comparison with theory for clean Pd(111) was limited to energies below 200 eV. It covered cumulative energy ranges of 330 eV, 590 eV, and 630 eV for the data at (θ, ϕ) = (0 °, 0 °), (5 °, 0 °), and (5 °, 180 °), respectively. For CO/Pd(111), the cumulative energy ranges compared with theory were 610 eV, 1170 eV, and 1080 eV for (θ, ϕ) = (0 °, 0 °), (5 °, 0 °), and (5 °, 180 °), respectively.

3. Theory

We have chosen established multiple-scattering methods to calculate LEED intensities[36]. For most trial structures Renormalized Forward Scattering was used to stack the metal layers and the separate C and O overlayers. To investigate possible CO-induced lateral distortions of the topmost metal layer as well as short C-O distances, the Combined Space Method was applied. The C, O, and topmost metal atoms were treated as a single composite layer with Matrix Inversion.

The phase shifts describing the electron scattering by palladium atoms were obtained from a band-structure potential[37], used previously for LEED studies of Pd(100) and CO on Pd(100)[10,11]. The CO scattering phase shifts are the same as used previously in studies of CO adsorbed on various metal surfaces[1–3,9–11]. The spherical-wave expansion was cut off at l_{max}=7, with the exception of the case of lateral substrate distortions, for which l_{max}=6 was used. The imaginary part of the muffin-tin potential was held constant at 5eV. The metal Debye temperature was uniformly chosen as the bulk value (270K), divided by 1.2 to represent enhanced surface vibrations. The C and O atoms were given the mean square vibration amplitudes of the bulk Pd atoms, multiplied by 2 to take a probable surface enhancement into account.

For the comparison between experiment and theory, a set of five R-factor formulas and their average was used, as described previously and used by us in many prior LEED analyses[1–3].

4. Analysis and Results

4.1. Clean Pd(111) Surface Structure

In an initial analysis of the clean Pd(111) surface structure, we allowed the topmost layer spacing d_{12} to relax. We found it to expand by about 0.05Å using both the normal and the off-normal incidence data. This unexpected behavior prompted us to investigate a multilayer relaxation. To that end we allowed the two top spacings d_{12} and d_{23} to relax independently of each other and independently of the deeper spacings, which were all varied together (d_{34}=d_{45}= ...). At our LEED energies, very little sensitivity to d_{45} and deeper spacings exists. The ranges of variation were as follows, where we refer the changes Δd_{mn} to the bulk value 2.2462Å, and use positive values for expansions:

$$-0.05 \leq \Delta d_{12} \leq 0.10\text{Å } \textit{in steps of } 0.05\text{Å}$$

$$-0.20 \leq \Delta d_{23} \leq 0.10\text{Å } \textit{in steps of } 0.05\text{Å}$$

$$0.0 \leq \Delta d_{34} = \Delta d_{45} = \Delta d_{56} = \cdots \leq 0.10\text{Å } \textit{in steps of } 0.05\text{Å}$$

An R-factor contour plot for normal incidence data is presented in Fig.2. Besides changes in interlayer spacing, we also investigated possible changes in layer stacking at the clean surface, allowing the stacking to change from face-center cubic (fcc) to hexagonal close-packed (hcp): (A) ideal fcc crystal structure in the surface region (ABCABC...stacking); (B) ideal hcp structure in the surface region (ABABA...stacking); (C) fcc monolayer on hcp structure (ABCBCB...stacking); and (D) hcp monolayer on fcc structure(ABACBAC...stacking).

We have found that the ideal fcc stacking sequence (A) is favored and that the optimal interlayer spacings are: Δd_{12}= +0.03±0.03Å, Δd_{23}= −0.03± 0.03Å, and Δd_{34}= Δd_{45} = +0.05±0.03 Å. The optimum muffin-tin zero level was V_0= 8.0±0.5 eV below vacuum. This structure yields a five-R-factor average of R=0.12 (using the normal-incidence data only, since the final optimization was not performed with off-normal data); the corresponding Zanazzi-Jona and Pendry R-factor values are approximately 0.09 and 0.22, respectively.

4.2. Pd(111)-($\sqrt{3}$x$\sqrt{3}$)R30°-CO Surface Structure

We have examined a variety of adsorbed structures for CO in the ($\sqrt{3}$x$\sqrt{3}$)R30° unit cell as listed in Table 1 (additionally an hcp-terminated substrate was tested). They all assume one CO molecule per unit cell with C-O axis perpendicular to the surface. For the first set of analyses (A,B,C,D), the ideal substrate structure was assumed and the CO adsorption sites, the carbon-oxygen bond length, and the perpendicular metal-carbon distance were varied independently. The favored structure among these has CO at a fcc hollow site with a carbon-oxygen bond length of ~1.1Å and a perpendicular metal-carbon distance of ~1.3Å; this was found with both the normal-incidence data and the off-normal-incidence data. The results of these analyses are shown in Table 2. After settling the CO adsorption site to fcc-hollow, we used the normal incidence data to examine possible substrate relaxations, since we had observed a slight relaxation for the clean Pd(111) surface. In trial(E), changes of the perpendicular interlayer spacings down to the 3rd layer slightly improved the R-factor. R-factor

contour plots for these analyses (trial E) are presented in Fig.3. Finally, in trial(F), we allowed a lateral displacement of the atoms in the 1st substrate layer to investigate the possibility of a CO-induced metal reconstruction. The displacements were made compatible with the $(\sqrt{3}x\sqrt{3})R30^\circ$ unit cell and kept of the highest symmetry, as illustrated in Fig.4. Such displacements, however, worsened the R-factor ($\Delta R \sim 0.1$ for a displacement of $\Delta r = 0.1$Å).

Consequently, the LEED comparisons strongly favor the fcc-hollow site for CO adsorbed on an unreconstructed Pd(111) substrate. The optimal structural parameters are: C-O bond length d_{C-O} of 1.15±0.05Å, perpendicular metal-carbon distance d_{Pd-C} of 1.29±0.05Å (i.e. metal-carbon bond length b_{Pd-C} of 2.05 ± 0.04 Å), interlayer spacing between 1st and 2nd metal layers (d_{12}) of 2.3862±0.05Å ($\Delta d_{12} = +0.14 \pm 0.05$Å), and interlayer spacing between 2nd and 3rd layers (d_{23}) of 2.2462±0.05Å ($\Delta d_{23} = 0.00 \pm 0.05$Å). The structural result is illustrated in Fig.4. The optimal muffin-tin zero level, assumed layer-independent, is found to be 6±1eV below vacuum. The minimized value of the five-R-factor average is 0.30, while the corresponding Zanazzi-Jona and Pendry R-factor values are 0.56 and 0.55 (using the normal-incidence data only). Although the final R-factor values are too high to call the structure solved, they are closely comparable to values obtained for some other structures analyzed recently: for example, Pt(111)-c(4x2)-2CO[1] with R(average)=0.29, R(Zanazzi-Jona)=0.50, R(Pendry)=0.61, and Rh(111)-c($2\sqrt{3}$x4)*rect*-C_6H_6+CO[15] with R(average)=0.31, R(Zanazzi-Jona)=0.40, R(Pendry)=0.66. In view of our extensive database and the many structural models tested, we feel that we have identified the major

ingredients of this structure.

5. Discussion

5.1. Clean Pd(111) Surface Structure

The structure of clean Pd(111) which we obtain has the ideal bulk structure within ~0.05Å. The 5 average R-factor value is small (0.12), indicating good agreement between theory and experiment. The small deviations of our optimal structural values for the interlayer spacings from the ideal structure are:

$$\Delta d_{12} = +0.03 \pm 0.03 \AA \ \ [+1.3 \pm 1.3\%]$$

$$\Delta d_{23} = -0.03 \pm 0.03 \AA \ \ [-1.3 \pm 1.3\%]$$

$$\Delta d_{34} = +0.05 \pm 0.03 \AA \ \ [+2.2 \pm 1.3\%]$$

$$\Delta d_{45} = +0.05 \pm 0.03 \AA \ \ [+2.2 \pm 1.3\%]$$

(positive/negative values correspond to expansion/contraction).

The average spacing expansion of the near surface region (from the 1st layer to the 5th layer) is ~1.1% with respect to the bulk value.

Since Pd(111) is a close-packed face, one may expect an ideal surface structure. Indeed, almost all the close-packed metal surfaces appear to have the ideal, unrelaxed structure or perhaps a slightly contracted structure. According to a recent surface structure tabulation[38], possibly the only exceptions until now were the cases of Al(111) and Pt(111). For Al(111), there are contradictory results for

the topmost interlayer spacing: Two results show expansions (+2.2%, +5%), two other results show contractions (−3%, −8%), and some show unrelaxed structures. For Pt(111), several results show expansions (+0.5%, +1%, +1.3%, +1.5%, +1.5%), and others show ideal structures.

In view of the easy absorption of hydrogen in bulk palladium and of the resulting difficulty of keeping the Pd(111) surface free of hydrogen, it is possible that the small relaxations seen at this surface are due to hydrogen in the surface region. It is well known that the Pd bulk lattice expands as the hydrogen concentration in the bulk increases[39,40]. For example, when the H/Pd ratio is ~0.6, where the α phase and the β phase coexist, the lattice expansion is ~3.5%. Most hydrogen is presumably located in the octahedral interstitial sites[39,40]. Regarding the surface properties of hydrided palladium, Christmann *et al.*[29] have exposed a Pd(111) crystal to more than 100L of hydrogen, and observed Bragg peak shifts corresponding to an average expansion of the interlayer spacings by $\sim 2\%$ in the surface region. The occupation of subsurface sites by hydrogen on Pd(111) has been suggested by W. Eberhardt *et al.*[41], F.Greuter *et al.*[42], T.E. Felter *et al.*[43,44], and S.M. Foiles *et al.*[45]. These studies indicate that octahedral sites between the first and second layers could be the most favorable subsurface sites. This would be consistent with the small topmost spacing expansion which we see.

We should also mention here that a dynamical LEED analysis of clean Pd(100) has shown similar results[10,11]. The structure is close to ideal, but the optimal topmost spacing seems to be slightly expanded: $\Delta d_{12} = +2.5 \pm 2.5\%$.

5.2. Pd(111)-($\sqrt{3}$x$\sqrt{3}$)R30°-CO Surface Structure

Our analysis has found the adsorption site of CO to be the fcc-hollow site. The optimal interlayer spacings and bond lengths are:

$$d_{C-O} = 1.15\mathring{A} \pm 0.05\mathring{A}$$

$$d_{Pd-C} = 1.29\mathring{A} \pm 0.05\mathring{A}$$

$$b_{Pd-C} = 2.05\mathring{A} \pm 0.04\mathring{A}$$

$$\Delta d_{12} = +0.14 \pm 0.05\mathring{A} \quad [+6.2 \pm 2.2\%]$$

$$\Delta d_{23} = 0.00 \pm 0.05\mathring{A} \quad [0.0 \pm 2.2\%]$$

Adsorption site: The binding site which we obtain for a third of a monolayer of CO adsorbed on Pd(111), namely the hollow site, confirms the expectations based on vibrational spectroscopy[12,13]. We have no evidence of the mixture of domains of bridge-site CO and hollow-site CO which has been proposed based on SIMS data[20].

The bonding of CO to transition metal surfaces can be explained by the donation-backdonation model originally proposed by Blyholder[46]: the CO 5σ orbitals donate electrons to the metal and the metal back-donates electrons to the CO $2\pi^*$ orbitals. Theoretical investigations to explain the stability of CO adsorbed at a hollow site of Pd(111) using quantum mechanical calculations have been pursued recently. Anderson *et al.*[47] have compared the chemisorption property of CO on palladium and platinum, and have proposed that the higher position of the Pd valence band compared to that of Pt, and the consequent enhancement of

the backdonation, are responsible for CO on Pd(111) preferring hollow-site adsorption. More recently, Van Santen[48] has suggested that the d-band half-width is also an important factor affecting the CO adsorption site. Palladium has a d-band half-width of 2.93eV, which is narrower than that of Pt or Rh, both of which favor top-site adsorption of CO. The narrower d-band implies a decreased interaction between CO and palladium d electrons. Both the higher position of the valence band and the narrower d-band half-width for palladium seem to enhance the CO bonding in highly coordinated sites.

Total-energy calculations show little difference in binding energy between the two types of hollow sites on Pt(111)[49]; the same holds presumably also on Pd(111). Nevertheless, the LEED result clearly shows a preference for the fcc-type hollow site. A fcc-type hollow site is located right overhead of a octahedral subsurface site where, as we mentioned before, hydrogen may sit. There may thus be a correlation between CO and hydrogen subsurface sites.

Bond lengths: There is a correlation between the bond lengths of adsorbed CO and the adsorption sites, as reported by D.F. Ogletree *et al.*[1] based on LEED data: both M-C bond lengths and C-O bond lengths increase as the metal coordination number increases. Our data for CO on Pd(111) fit this scheme. Also, the Pd-C and the C-O bond lengths obtained agree well with the values found for the face-bridging CO in high-nuclearity metal carbonyl clusters[50]: the M-C and the C-O bond lengths range in such clusters from 2.00 to 2.23Å and from 1.15 to 1.21Å, respectively.

6. Conclusions

The structure of Pd(111) surface is confirmed to be almost equal to that of the bulk structure, within $\sim$ 0.05Å with good R-factor values. Small deviation from the ideal bulk value are found, which might indicate surface relaxations due to hydrogen in the near surface region.

The structure of CO adsorbed at a coverage of 1/3 monolayer on Pd(111) has also been analyzed. All CO molecules are favored to occupy fcc-type hollow sites with a $(\sqrt{3}x\sqrt{3})R30^\circ$ surface periodicity. The C-O and Pd-C bond distances obtained agree well with the values for three-fold coordinated CO in high-nuclearity metal carbonyl clusters.

Acknowledgements

We thank Dr. D. Frank Ogletree for fruitful discussions and assistance. This work was supported by the Director, Office of Energy Research, Office of Basic Energy Sciences, Materials Sciences Division, of the U.S. Department of Energy under contract No. DE-AC03-76SF00098. We also acknowledge supercomputer time provided by the Office of Energy Research of the U.S. Department of Energy. H. Ohtani gratefully acknowledges financial support from IBM Japan.

References

1 D.F. Ogletree, M.A. Van Hove, and G.A. Somorjai, Surf. Sci. **173**, 351 (1986).

2 R.J. Koestner, M.A. Van Hove, and G.A. Somorjai, Surf. Sci. **107**, 439 (1981).

3 M.A. Van Hove, R.J. Koestner, J.C. Frost, and G.A. Somorjai, Surf. Sci, **129**, 482 (1983).

4 G. Michalk, W. Moritz, H. Pfnür, and D. Menzel, Surf. Sci. **129**, 92 (1983).

5 S. Andersson and J.B. Pendry, Phys. Rev. Lett. **43**, 363 (1979).

6 S. Andersson and J.B. Pendry, J. Phys. **C13**, 3547 (1980).

7 M.A. Passler, A. Ignatiev, F. Jona, D.W. Jepsen, and P.M. Marcus, Phys. Rev. Lett. **43**, 360 (1979).

8 K. Heinz, E. Lang, and K. Müller, Surf. Sci. **87**, 595 (1979).

9 S.Y. Tong, A. Maldonado, C.H. Li, and M.A. Van Hove, Surf. Sci. **94**, 73 (1980).

10 R.J. Behm, K. Christmann, G. Ertl, M.A. Van Hove, P.A. Thiel, and W.H. Weinberg, Surf. Sci. **88**, L59 (1979).

11 R.J. Behm, K. Christmann, G. Ertl, and M.A. Van Hove, J. Chem. Phys. **73**, 2984 (1980).

12 A.M. Bradshaw and F.M. Hoffmann, Surf. Sci. **72**, 513 (1978).

13 F.M. Hoffmann and A. Ortega, in: Proc. Intern. Conf. on Vibrations in Adsorbed Layers, Jülich 1978, KFA Reports - Jülich, Conf. 26 (1978) p.128.

14 C.M. Mate and G.A. Somorjai, Surf. Sci. **160**, 542 (1985).

15 M.A. Van Hove, R.F. Lin, and G.A. Somorjai, J. Amer. Chem. Soc. **108**, 2532 (1986).

16 R.F. Lin, G.S. Blackman, M.A. Van Hove, and G.A. Somorjai, Acta Crystallographica B (submitted).

17 G. Ertl and J. Koch, Z. Naturforsch. **25a**, 1906 (1970).

18 G. Ertl and J. Koch, in: Adsorption-Desorption Phenomena, ed. F. Ricca (Academic Press, New York, 1972) p.345.

19 H. Conrad, G. Ertl, and J. Küppers, Surf. Sci. **76**, 323 (1978).

20 A. Brown and J.C.Vickerman, Surf. Sci. **124**, 267 (1983).

21 A. Noordermeer, G.A. Kok, and B.E. Nieuwenhuys, Surf. Sci. **165**, 375 (1986).

22 A. Noordermeer, G.A. Kok, and B.E. Nieuwenhuys, Surf. Sci. **172**, 349 (1986).

23 F.P. Netzer and M.M. El Gomati, Surf. Sci. **124**, 26 (1983).

24 J.P. Bibérian and M.A. Van Hove, Surf. Sci. **138**, 361 (1984).

25 T. Engel, J. Chem. Phys. **69**, 373 (1978).

26 H. Conrad, G. Ertl, J. Küppers, S.W. Wang, K. Gérard, and H. Haberland, Phys. Rev. Lett. **42**, 1082 (1979).

27 D.R. Lloyd, C.M. Quinn, and N.V. Richardson, Solid State Comm. **20**, 409 (1976).

28 R. Miranda, K. Wandelt, D. Rieger, and R.D. Schnell, Surf. Sci. **139**, 430 (1984).

29 K. Christmann, G. Ertl, and O. Schober, Surf. Sci. **40**, 61 (1973).

30 F. Maca, M. Scheffler, and W. Berndt, Surf. Sci. **160**, 467 (1985).

31 Y. Kuk, L.C. Feldman, and P.J. Silverman, J. Vac. Sci. Technol. A, **1**, 1060 (1983).

32 Y. Kuk, L.C. Feldman, and P.J. Silverman, Phys. Rev. Lett. **50**, 511 (1983).

33 D.F. Ogletree, G.A. Somorjai, and J.E. Katz, Rev. Sci. Instruments, **57**, 3012 (1986).

34 L.L. Kesmodel and G.A. Somorjai, Phys. Rev. **B11**, 630 (1975).

35 T.M. Gentle, Ph.D. Thesis, University of California, Berkeley (1984).

36 M.A. Van Hove and S.Y. Tong, "Surface Crystallography by LEED" Springer (Heidelberg) 1979.

37 V.L. Moruzzi, J.F. Janak, and A.R. Williams, "Calculated Electronic Properties of Metals", Pergamon (New York) 1978.

38 J.M. McLaren, J.B. Pendry, R.J. Rous, D.K. Saldin, G.A. Somorjai, M.A. Van Hove, and D.D. Vvedensky, "Surface Crystallographic Information Service)" Reidel, Dordrecht, to be published.

39 F.A. Lewis, "The Palladium Hydrogen System", Academic Press (1967) and references therein.

40 E. Wicke, H. Brodowsky, and H. Zühner, in: Hydrogen in Metals II, Ed. G. Alefeld and J. Völkl (Springer-Verlag, Berlin, 1978) and references therein.

41 W. Eberhardt, F. Greuter, and E.W. Plummer, Phys. Rev. Lett. **46**, 1085 (1981).

42 F. Greuter, W. Eberhardt, J. DiNardo, and E.W. Plummer, J. Vac. Sci. Tec. **18**, 433 (1981).

43 T.E. Felter, S.M. Foiles, M.S. Daw and R.H. Stulen, Surf. Sci. **171**, L379 (1986).

44 T.E. Felter and R.H. Stulen, J. Vac. Sci. Tec. **A3**, 1566 (1985).

45 S.M. Foiles and M.S. Daw, J. Vac. Sci. Tec. **A3**, 1565 (1985).

46 G. Blyholder, J. Phys. Chem. **68**, 2772 (1964).

47 A.B. Anderson and M.K. Awad, J. Am. Chem. Sci. **107**, 7854 (1985).

48 R.A. van Santen, Faraday Symp. Chem. Soc. **21**, in press.

49 N.K. Ray and A.B. Anderson, Surf. Sci. **125**, 803 (1983).

50 P. Chini, G. Longoni, and V.G. Albano, Adv. Organomet. Chem. **14**, 285 (1976).

TABLE 1. Test structures for Pd(111)-($\sqrt{3}$x$\sqrt{3}$)R30°-CO

(the notation $x_1(\Delta x)x_2$ indicates a variation range x_1 to x_2 and a step Δx)

	Adsorption site	d_{C-O}(Å)	d_{Pd-C}(Å)	Δd_{12}(Å)	Δd_{23}(Å)	Δr^*(Å)
A	top	1.1(.1)1.4	1.7(.1)2.2	0.0	0.0	0.0
B	fcc-hollow	1.1(.1)1.4	1.2(.1)1.7	0.0	0.0	0.0
C	bridge	1.1(.1)1.4	1.3(.1)1.8	0.0	0.0	0.0
D	hcp-hollow	1.1(.1)1.4	1.2(.1)1.7	0.0	0.0	0.0
E	fcc-hollow	1.15	1.1(.1)1.4	−.2(.1).3	−.3(.1).1	0.0
F	fcc-hollow	1.15	1.1(.1)1.4	−.3(.1).2	−.4(.1)0.0	0.1,−0.1

* lateral displacement in the 1st layer Pd atoms (See Fig.4), including either expansion away from CO ($\Delta r>0$) or contraction toward CO ($\Delta r<0$)

TABLE 2. R-factor comparison for CO adsorbed at different sites, keeping the substrate bulk-like. (the best geometry here is not interpolated between calculated grid points)

model		Best geometry		5-Average R-Factor
		d_{C-O}(Å)	d_{Pd-C}(Å)	
A	top	1.4	2.0	0.4123
B	fcc-hollow	1.1	1.3	0.3004
C	bridge	1.1	1.7	0.3771
D	hcp-hollow	1.2	1.6	0.4127

TABLE 3. Structure Result in Format of Surface Crystallographic Information Service (SCIS)[38]

SURFACE: Substrate Face: Pd(111)

Surface Pattern: (1x1), (1,0/0,1)

STRUCTURE: Bulk Structure: fcc; Temp: 300K

REFERENCE UNIT CELL: a=2.75Å; b=2.75Å; A(a,b)=60°

Layer	Atom	Atom Positions		Normal Layer Spacing
S1	Pd	0.0	0.0	2.28
S2	Pd	0.3333	0.3333	2.22
S3	Pd	0.6667	0.6667	2.30
S4	Pd	0.0	0.0	2.30

2D Symmetry: p3m1

Thermal Vibrations: Debye Temp=225K

R-factor: R_{VHT}=0.12 R_{ZJ}=0.09 R_P=0.22

TABLE 4. Structure Result in Format of Surface Crystallographic Information Service (SCIS)[38]

SURFACE: Substrate Face: Pd(111); Adsorbate CO;

Surface Pattern: $(\sqrt{3}x\sqrt{3})R30°$, (2,1/1,2)

STRUCTURE: Bulk Structure: fcc; Temp: 300K; Adsorbate State: Molecular;

Coverage: 1/3 (CO/Pd)

REFERENCE UNIT CELL: a=4.76Å; b=4.76Å; A(a,b)=120°

Layer	Atom	Atom Positions		Normal Layer Spacing
A1	O	0.0	0.0	1.15
A2	C	0.0	0.0	1.29
S1	Pd	0.3333	0.0	0.0
S2	Pd	0.0	0.3333	0.0
S3	Pd	0.6667	0.6667	2.39
S4	Pd	0.6667	0.0	0.0
S5	Pd	0.0	0.6667	0.0
S6	Pd	0.3333	0.3333	2.25

2D Symmetry: p3m1

Thermal Vibrations: Debye Temp=225K with double amplitude for surface atoms;

R-factor: R_{VHT}=0.30 R_{ZJ}=0.56 R_P=0.55

Figure captions

1) (a) A photograph of the LEED pattern of the clean Pd(111) crystal surface. The incident electron energy is 70eV. Near-normal incidence is used.

   (b) A photograph of the LEED pattern of the $(\sqrt{3}x\sqrt{3})R30°$ structure formed when 1/3 monolayer of CO is adsorbed at room temperature on Pd(111). The incident electron energy is 65eV. Near-normal incidence is used.

2) Contour plot of the five-R-factor average as a function of two of the structural parameters for clean Pd(111). The parameters used are the interlayer spacing between the 1st and 2nd Pd layers, d_{12}, and that between the 2nd and 3rd Pd layers, d_{23}. The bulk spacing is 2.2462Å. Δd_{34} and Δd_{45} were held at +0.05Å for this plot. Muffin-tin zero at V_0= 8eV.

3) Contour plots for the five-R-factor average as a function of two of the structural parameters for Pd(111)-$(\sqrt{3}x\sqrt{3})R30°$-CO. The best R-factor value shown here is larger than the best R-factor value quoted in the text, because the contour plots are based on an approximation that allows lateral metal distortions.

   (a) The parameters used are the perpendicular distance between the top-layer Pd atoms and the fcc-hollow site carbon atoms (d_{Pd-C}), and the interlayer spacing between the 1st and 2nd Pd layers (d_{12}). The C-O bond length was held at 1.15Å for this plot.

   (b) The parameters used are the interlayer spacing between the 1st and 2nd Pd layers (d_{12}), and that between the 2nd and 3rd Pd layers (d_{23}). The perpendicular Pd-C distance d_{Pd-C} and the C-O bond length were held at 1.30Å and 1.15Å, respectively, for this plot.

4) The optimum structure for CO in the $(\sqrt{3}x\sqrt{3})R30°$ arrangement on the Pd(111) surface, as determined by dynamical LEED and R-factor analysis. The arrows in the top view indicate the lateral displacements of the Pd atoms which have been considered in the structure determination (see Table 1.F). The analysis showed, however, no indication of such displacement.

Pd(111) – (1×1)
T = 300K

LEED Pattern 70eV

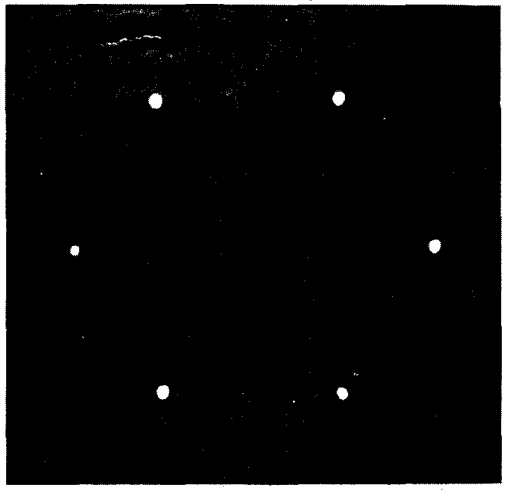

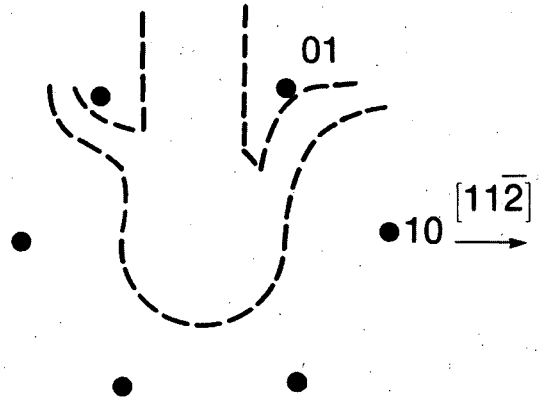

Pd(111) – ($\sqrt{3}\times\sqrt{3}$)R30° – CO
T = 300K

LEED Pattern 65eV

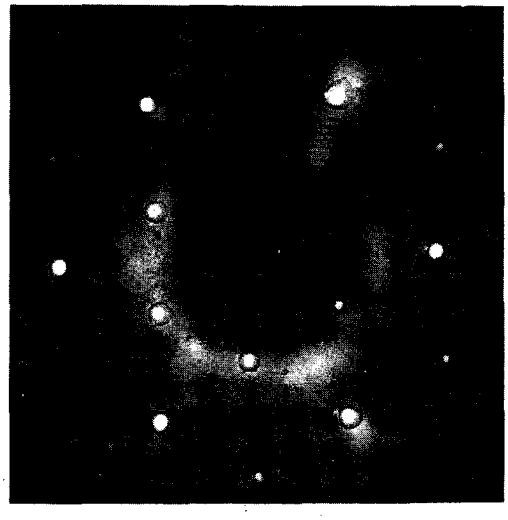

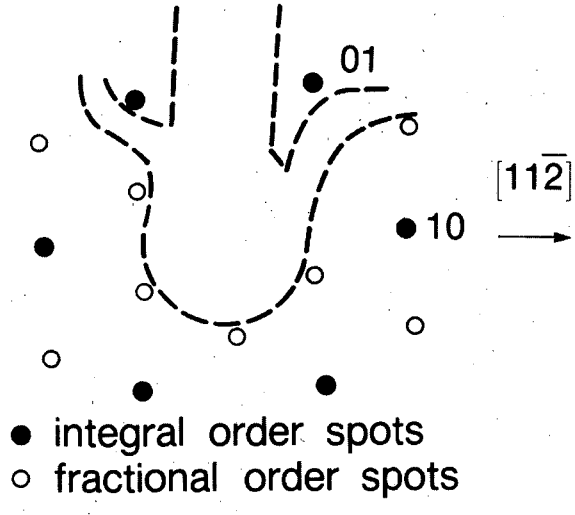

XBB 872-1089

Fig. 1

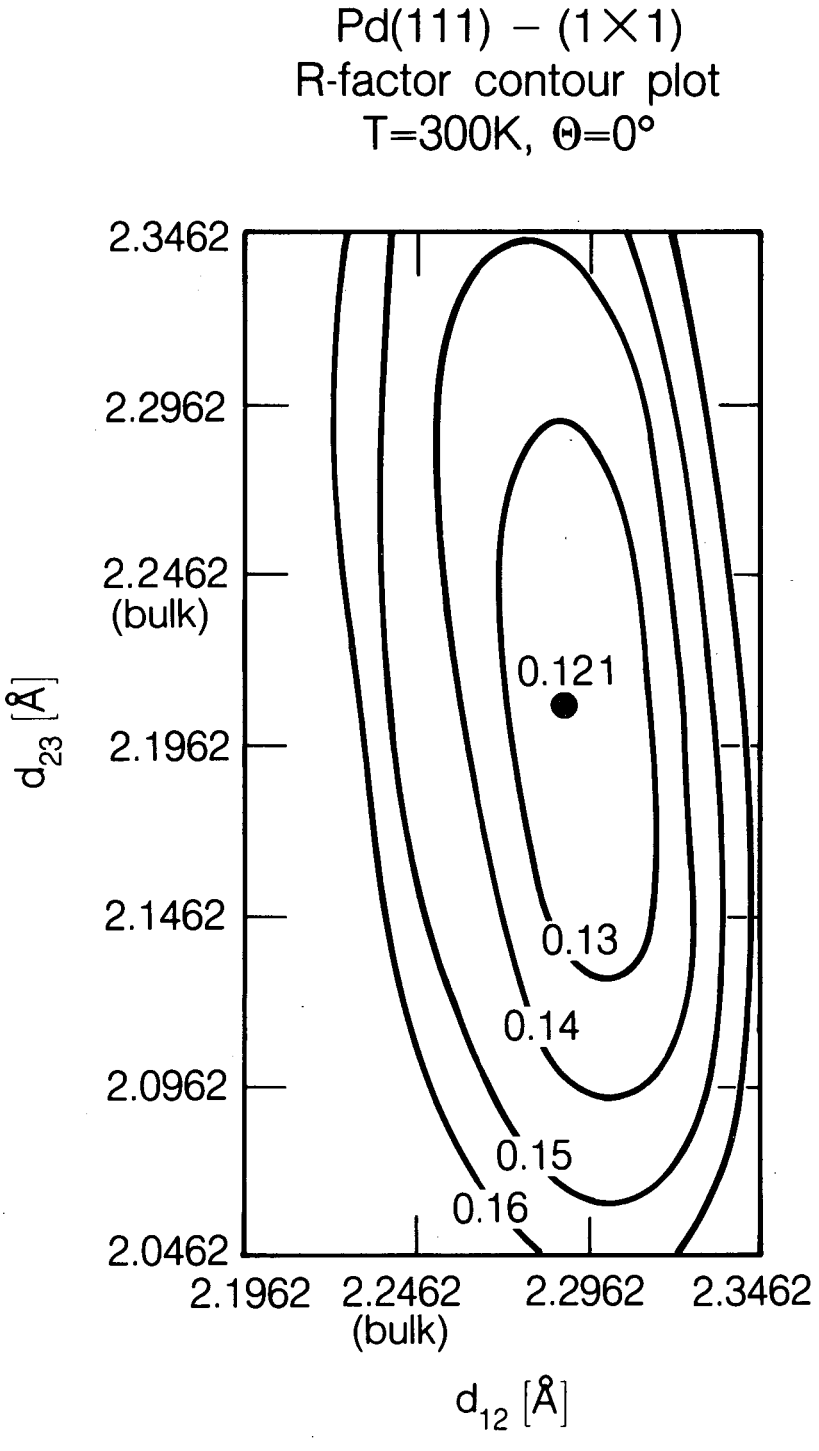

XBL 8611-9265

Fig. 2

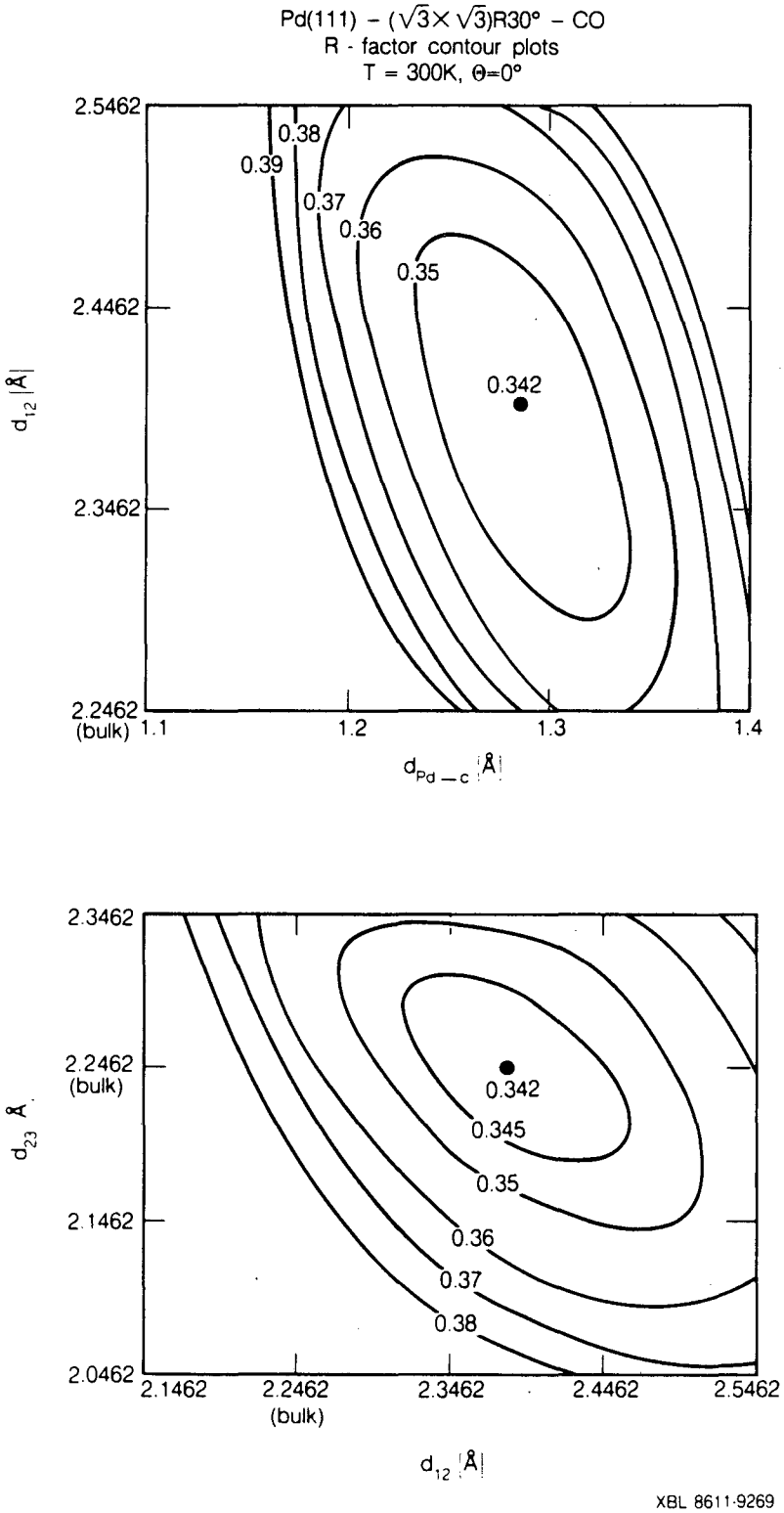
Pd(111) - (√3×√3)R30° - CO
R - factor contour plots
T = 300K, Θ=0°
2.5462
2.4462
2.3462
2.2462
(bulk)
1.1
1.2
1.3
1.4
0.38
0.39
0.37
0.36
0.35
0.342
d12 [Å]
dPd—c [Å]
2.3462
2.2462
(bulk)
2.1462
2.0462
0.342
0.345
0.35
0.36
0.37
0.38
2.1462
2.2462
(bulk)
2.3462
2.4462
2.5462
d23 Å
d12 [Å]
XBL 8611-9269

Fig. 3

The Structure of Pd(111) – $(\sqrt{3}\times\sqrt{3})R30°$ – CO

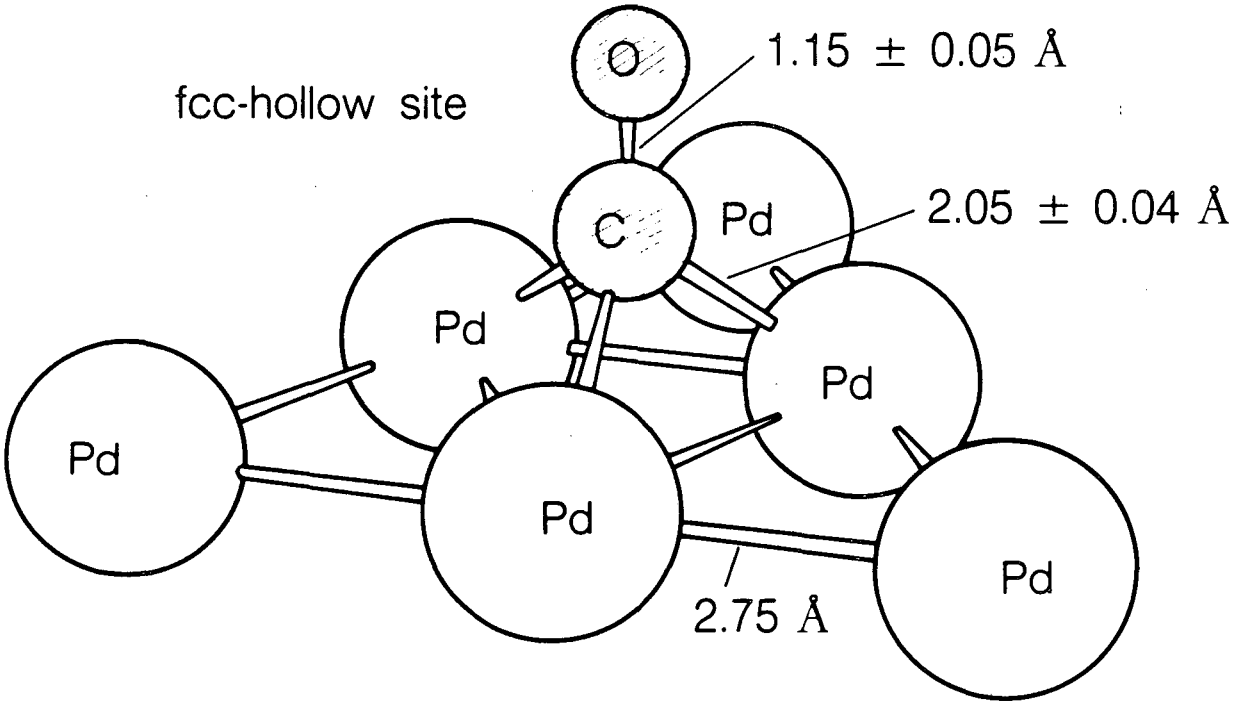

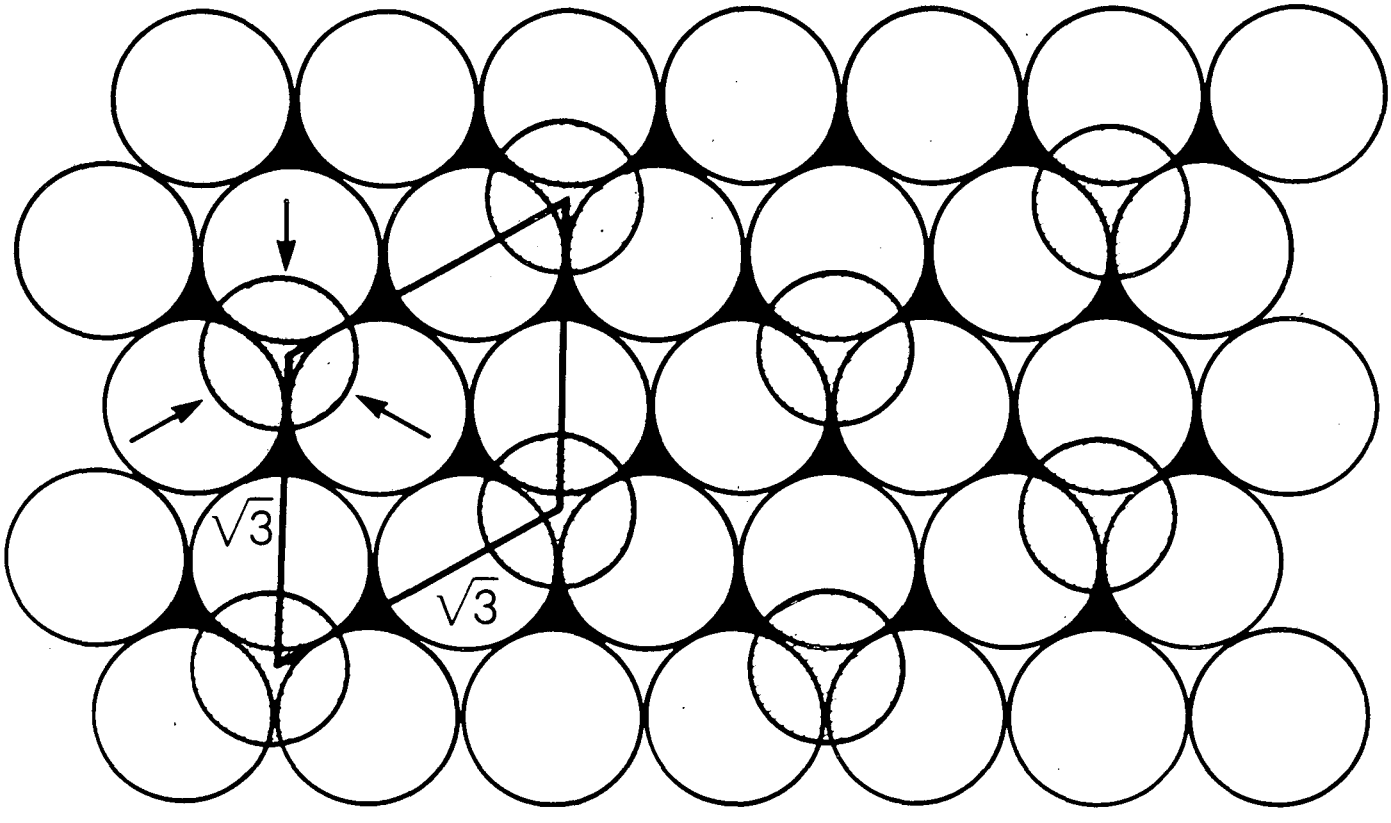

Top View

Fig. 4

XBL 8611-9263

LAWRENCE BERKELEY LABORATORY
TECHNICAL INFORMATION DEPARTMENT
UNIVERSITY OF CALIFORNIA
BERKELEY, CALIFORNIA 94720